Supporting Information: Lithium charge storage mechanisms of cross-linked triazine networks and their porous carbon derivatives

Kimberly A. See,[†,‡] Stephan Hug,[§,^,ﻩ] Katharina Schwinghammer,[§,^,ﻩ] Margaret A. Lumley,[‡,∥] Yonghao Zheng,[▽] Jaya M. Nolt,[∥] Galen D. Stucky,[†,‡,▽] Fred Wudl,[▽] Bettina V. Lotsch,[*,§,^,ﻩ] Ram Seshadri[*,†,‡,∥,▽]

[†]Mitsubishi Chemical – Center for Advanced Materials, University of California, Santa Barbara, CA 93106, USA
[‡]Department of Chemistry and Biochemistry, University of California, Santa Barbara, CA 93106, USA
[ﻩ]Nanosystems Initiative Munich and Center for Nanoscience, Schellingstr. 4, 80799 München, Germany
[§]Department Chemie, Ludwig-Maximilans-Universität München, Butenandtstr. 5-13, 81377 München, Germany
[^]Max-Planck-Institut für Festkörperforschung, Heisenbergstr. 1, 70569 Stuttgart, Germany
[∥]Materials Research Laboratory, University of California, Santa Barbara, CA 93106, USA
[▽]Materials Department, University of California, Santa Barbara, CA 93106, USA.

Preparation conditions and characterization of the PTI materials

The preparation of crystalline PTI (c-PTI) was first reported by Bojdys et al. via an ionothermal method.[1] Detailed characterization of the PTI materials determined that they consist of a 2D network of planar triazine units bridged by imides with the channels filled by Li^+ and Cl^-.[2] Long range order in the PTI materials can be modulated by varying the preparation procedure to produce amorphous PTI materials (a-PTI) which show no evidence of long range order in the X-ray diffraction (XRD) patterns.[3] It is known that a-PTI synthesized above 450 °C outperforms c-PTI as a photocatalyst suggesting that their electronic structures also change according to the morphology.[3] For this reason, both amorphous and crystalline PTI networks were evaluated as potential battery materials.

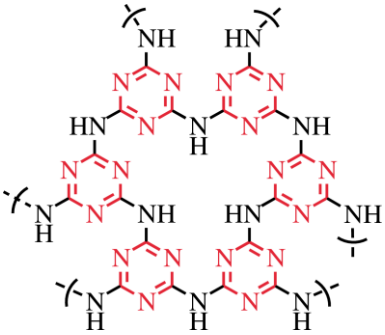

Figure S1. Poly(triazine imide), or PTI, is composed of 1,3,5-triazine bridged by secondary amines. These materials are well-defined with Li^+ and Cl^- ions occupying the channels (not shown). The N in the triazine or imide can be substituted, or "doped", with O or C depending on the synthesis procedure.

Both c-PTI and a–PTI materials were prepared for analysis in Li batteries. The synthesis of the c-PTI materials was performed according to previously published procedures.[1,2] Dicyandiamide (0.20 g, 2.38 mmol) and an eutectic mixture of lithium chloride (59.2 mol %, 0.90 g, 21.3 mmol) and potassium chloride (40.8 mol %, 1.01 g, 14.7 mmol) were hand ground with a mortar and pestle in a glove box. The reaction mixture was transferred in a dried quartz glass vessel, placed in a horizontal tube furnace, and heated under atmospheric Ar pressure at 6 °C min^{-1} to 400 °C. This temperature was held for 12 h and then cooled to room temperature at 20 °C min^{-1}. The resulting powders were then re-ground in Ar and transferred to a dried, thick-walled fused silica tube (15 mm OD and 11 mm ID) which was then evacuated and sealed at a length of 120 mm. The sealed ampule was placed in a horizontal tube furnace and heated at 1 °C min^{-1} to 600 °C in a second heating step and held at 600 °C for 24 h. After cooling to room temperature (6 °C min^{-1}), the ampule was broken and the sample was isolated and washed several times with boiling water to remove residual salt. The resulting material c-PTI was obtained as a brown powder (80 mg, 50%).

The synthesis of a-PTI and "doped" a-PTI (a-d-PTI), made by copolymerizing 4-amino-2,6-dihydroxy pyrimidine (4AP) with a-PTI, was carried out according to previous work by our group.[3] "Doped" here indicates that some of the N in the triazine or imide moieties are replaced by C or O. Dicyandiamide (0.50 g, 5.95 mmol) and an eutectic mixture of lithium chloride (59.2 mol %) and potassium chloride (40.8 mol %) were ground together in an Ar glove box. In the case of the copolymerized a-d-PTI samples, 4AP (0.72 g, 0.86 mmol) was added to the reaction mixture before grinding. The starting mixtures were transferred in a quartz glass vessel which was heated in a horizontal Ar-purged tube furnace at 12°C min^{-1} to the target temperature (indicated in Table 1). The temperature was held for 6 hr. followed by cooling to room

temperature (20 °C min^{-1}). The resulting powders were ground to achieve a homogenous product and heated again under the same conditions. Finally, the samples were isolated and washed several times with boiling water to remove residual salts. a-PTI yielded a yellow powder (0.15 g, 38%) and in the case of a-d-PTI-550, a dark orange colored product (0.16 g, 40%) was recovered.

The FTIR spectra clearly show strong signatures of the 1,3,5-triazine functionality indicating that well-defined triazine units are intact in the final materials at all synthesis temperatures.[3] The ratio of C to N in this family of materials is the lowest for all materials discussed here (Table S1). The crystalline PTI materials, denoted c-PTI, exhibit sharp reflections in the XRD indicative of long range order. The amorphous PTI materials, denoted a-PTI, show weak long range order in the XRD except layer stacking. This family of materials provides structures with well-defined triazine frameworks and varying long range order.

Table S1. Summary of synthesis conditions for poly(triazine imide) materials.

	Copolymerized ("doped") with 4AP	Syn. Temp (°C)
c-PTI-600	no	600
a-PTI-450	no	450
a-d-PTI-500	yes	500
a-d-PTI-550	yes	550

Table S2. Elemental analysis of the poly(triazine imide) and covalent triazine frameworks.

	N (wt%)	C (wt%)	H (wt%)	C/N (molar ratio)
c-PTI-600	46.8	29.8	1.5	0.74
a-PTI-450	55.1	26.7	4.3	0.56
a-d-PTI-500	44.8	28.8	2.8	0.75
a-d-PTI-550	41.6	29.3	2.6	0.82
CTF1-400-1	18.60	70.20	3.30	4.4
CTF1-400-10	14.63	70.34	3.62	5.6
CTF1-500	12.39	76.45	1.34	7.2
CTF1-600	10.37	79.16	1.34	5.3
bipy-CTF-400	20.42	58.85	4.08	3.3
bipy-CTF-500	16.42	63.14	2.67	4.5
bipy-CTF-600	13.61	67.53	2.01	5.8

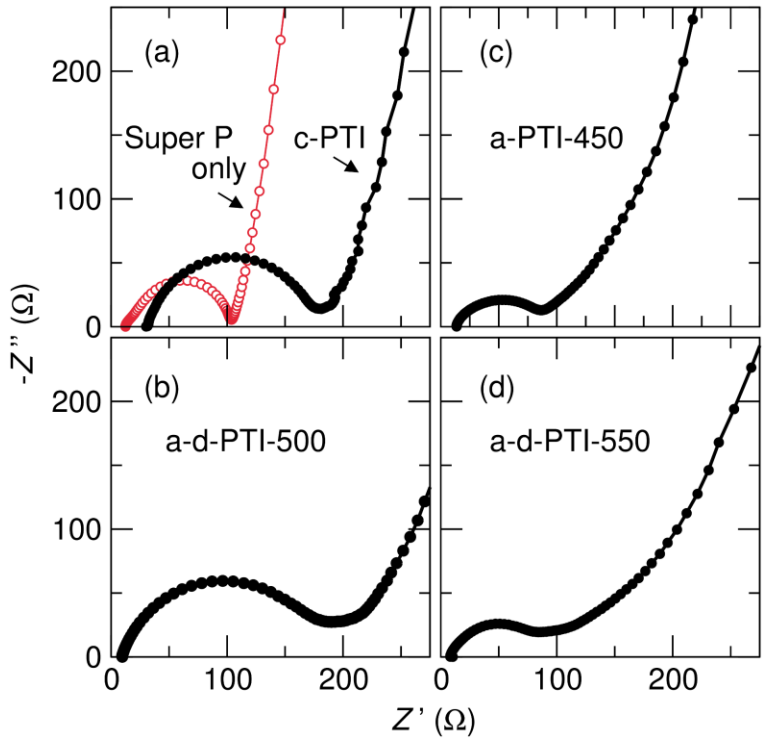

Figure S2. The Nyquist plots of the PTI cells before cycling do not show anomalously high resistances suggesting that the electrode conductivity does not limit capacity. The plot of a Super P only cell is shown in (a) for reference.

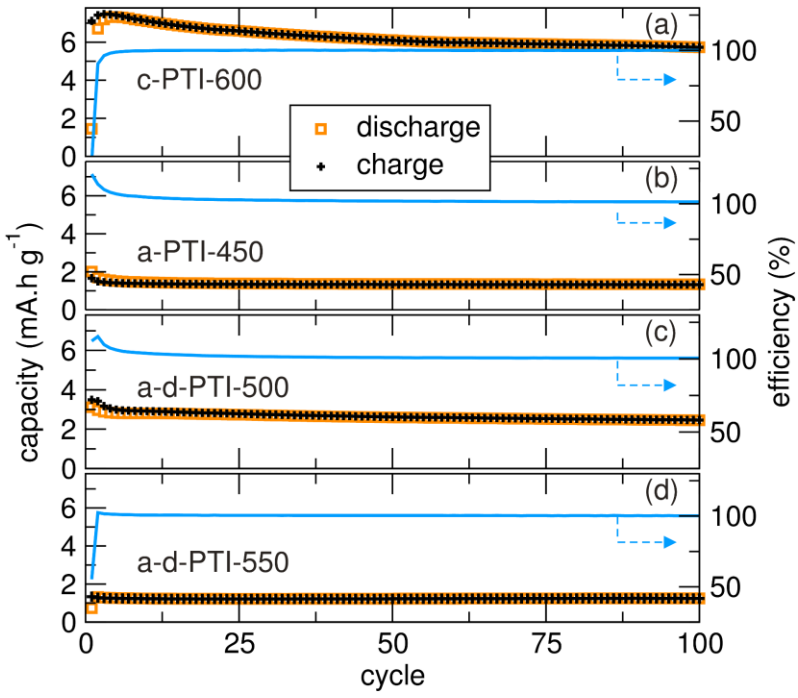

Figure S3. The PTI networks show very low capacities when cycled at 0.1 A g^{-1} from 1.5 V to 4.5 V in 1 M $LiPF_6$ in EC/DMC electrolyte vs. Li metal. (a) The c-PTI-600 material exhibits slightly higher capacities than the amorphous materials (a-PTI and a-d-PTI) synthesized at (b) 450 °C, (c) 500 °C, and (d) 550 °C.

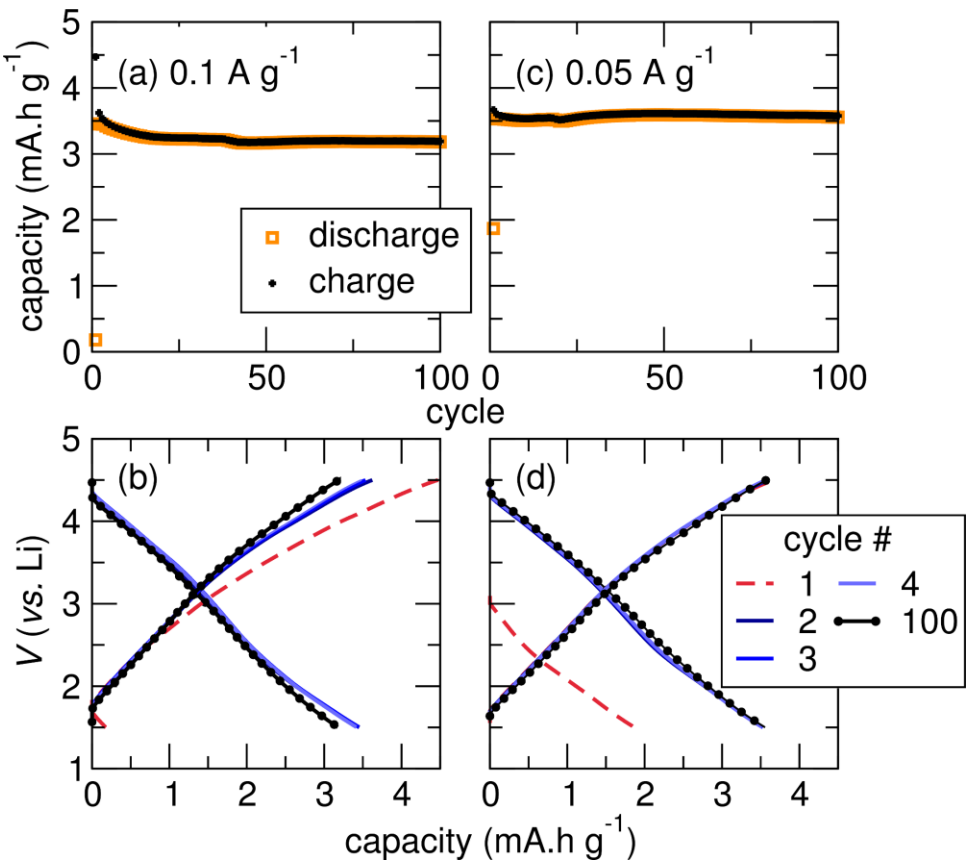

Figure S4. Control cells cycled with only the conductive carbon additive Super P (5 mg) at 0.1 A g^{-1} (left column) and 0.05 A g^{-1} (right column) from 1.5 V (*vs.* Li) to 4.5 V (*vs.* Li). (a) The capacity of the Super P only cells is below 5 mA.h g^{-1} when cycled at 0.1 A g^{-1}. (b) The profiles are indicative of capacitive storage through double layer interactions only. (c) The capacity is also very low when cycled at 0.05 A g^{-1}, suggesting minimal rate dependence. (d) Again, these cells exhibit capacitive-like behavior as would be expected.

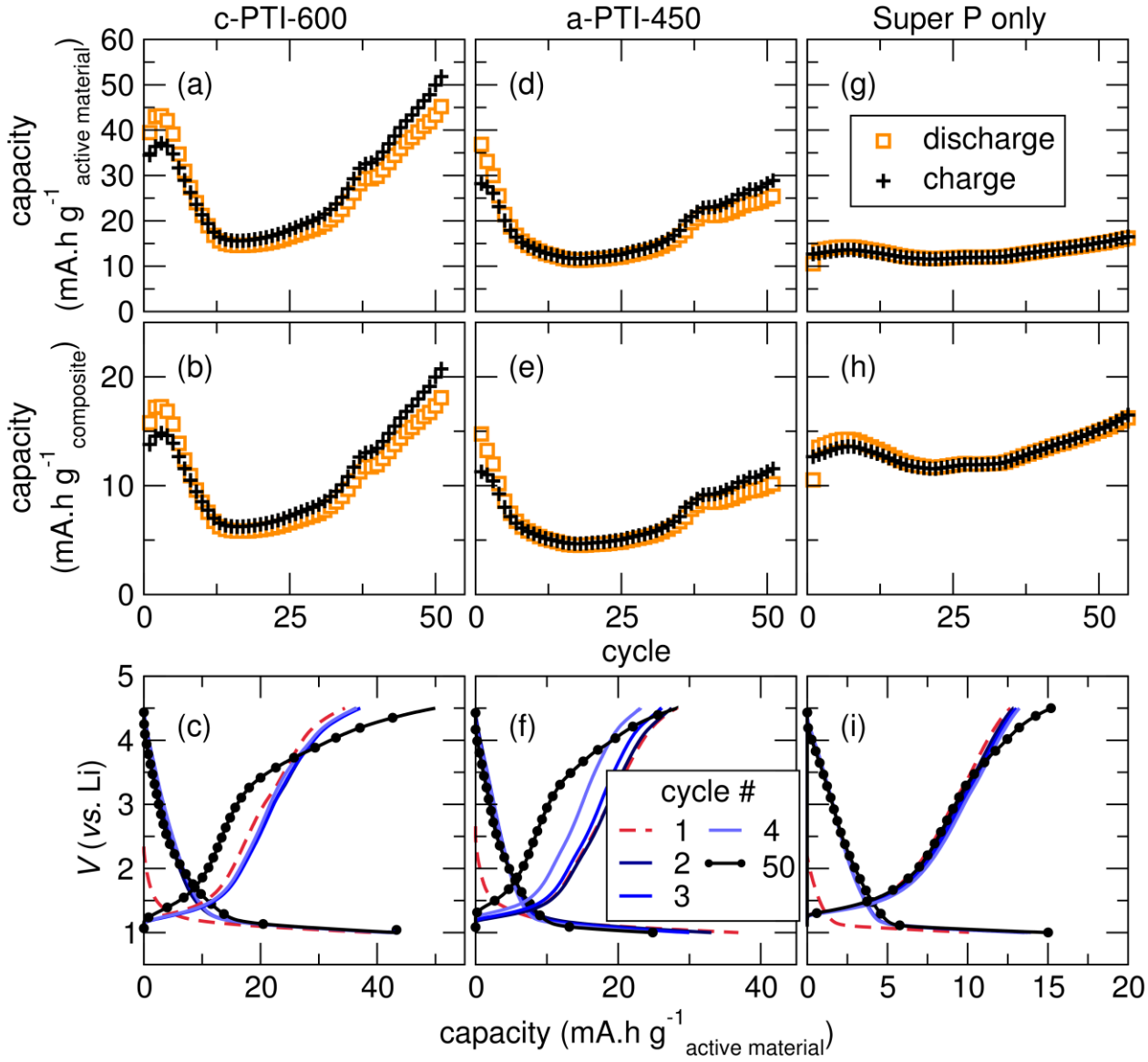

Figure S5. Galvanostatic cycling at 0.1 A g^{-1} of (a-c) c-PTI-600 and (d-f) a-PTI-450 from 1 V (*vs.* Li) to 4.5 V (*vs.* Li) along with the (g-i) Super P control cell. The two PTI materials that show promising plateaus near the end of discharge when cycled to 1.5 V (*vs.* Li) exhibit apparent capacity increases when cycled to 1.0 V (vs. Li) (top row). The capacity of c-PTI-600 increases from < 7 mA.h g^{-1} to (a) > 40 mA.h g^{-1} over 50 cycles. (c) The discharge and charge profiles of the c-PTI-600 exhibit reversible plateaus. (d) The capacity of a-PTI-450 also increases once it is cycled to lower voltages and exhibits a similar dip in the capacity at lower cycle numbers. (f) The profiles of the a-PTI-450 are similar to those of the c-PTI-600. (g) Because these cells were cycled to lower voltages, it is important to consider the activity of the carbon additive. The Super P control cell exhibits substantial reversible capacity in this voltage range, as well, contributing to the capacities seen in (a) and (d). (i) The discharge curve of Super P closely resembles those of the (c) c-PTI-600 and (f) a-PTI-450. Because of the activity of Super P at these potentials, it is only meaningful to consider the capacity normalized to the total mass of the electrode and compare it to the control cell, as shown in (b), (e), and (h). In this case, all three systems are relatively similar suggesting that the c-PTI-600 and a-PTI-450 do not contribute any substantial capacity to the Super P electrode.

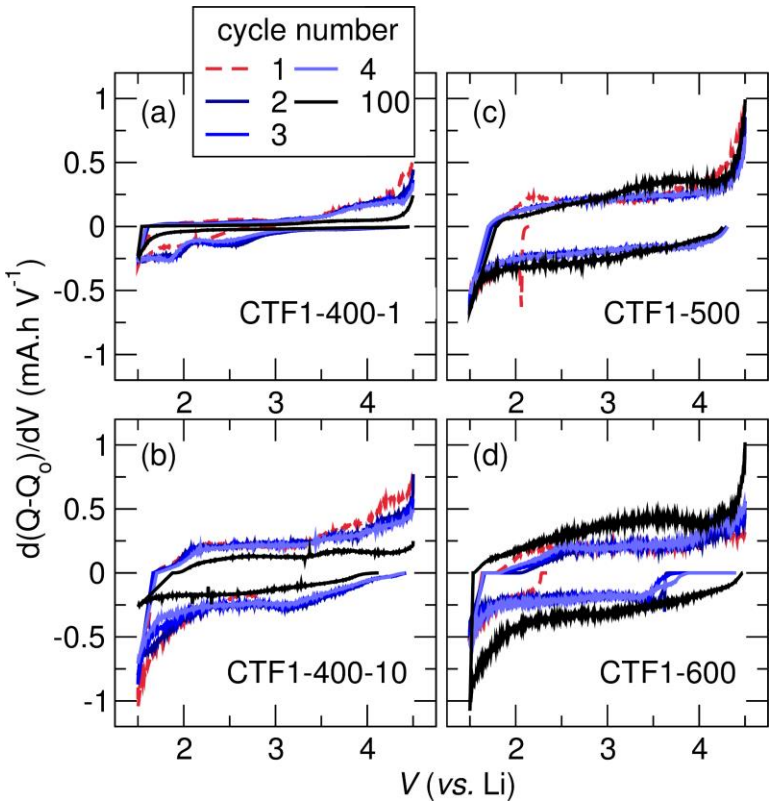

Figure S6. Differential capacity curves of the CTF1 materials cycled at 0.1 A g^{-1} from 1.5 V to 4.5 V (*vs.* Li) in 1 M $LiPF_6$ EC/DMC. (a) CTF1-400-1 shows two very broad peaks around 2.75 V (*vs.* Li) and 2.0 V (*vs.* Li) in the initial cycles suggesting the presence of two phase regions in the initial cycling, however, the capacity is very low. (b-d) The amorphous materials exhibit curves suggestive of capacitive mechanisms absent of any peaks.

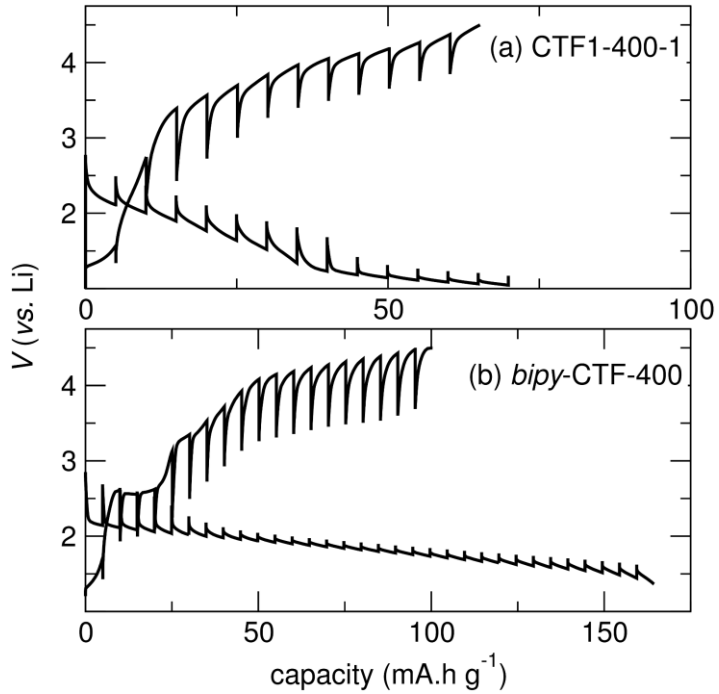

Figure S7. Galvanostatic intermittent titration technique (GITT) of the low temperature, rigid CTF networks showing the near-equilibrium discharge and charge profiles. (a) The discharge and charge profiles of the CTF1-400-1 exhibit a similar shape to those of the cell cycled at 0.1 A g^{-1} (Figure 4a) suggesting no kinetically limited processes are occurring. (b) The *bipy*-CTF-400 material exhibits a similar plateau in the discharge and charge as seen in the 0.1 A g^{-1} cycled cell (Figure 7a).

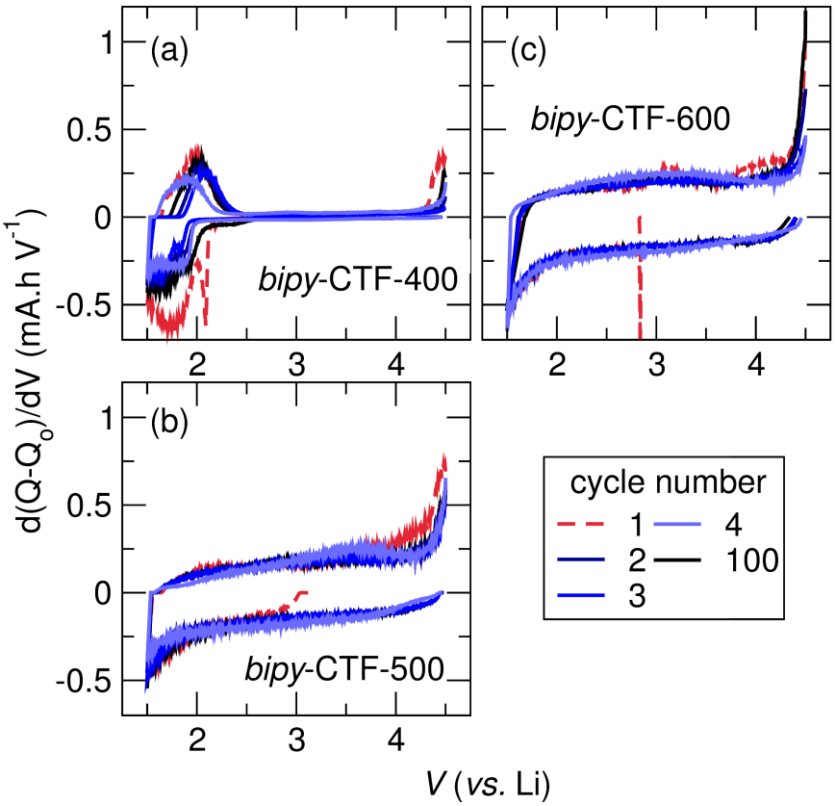

Figure S8. Differential capacity curves of the *bipy*-CTF materials cycled at 0.1 A g^{-1} from 1.5 V to 4.5 V (*vs.* Li) in 1 M $LiPF_6$ EC/DMC. The only material exhibiting peaks characteristic of two-phase regions is (a) *bipy*-CTF-400. (b-c) The amorphous materials exhibit open curves characteristic of capacitive charge storage.

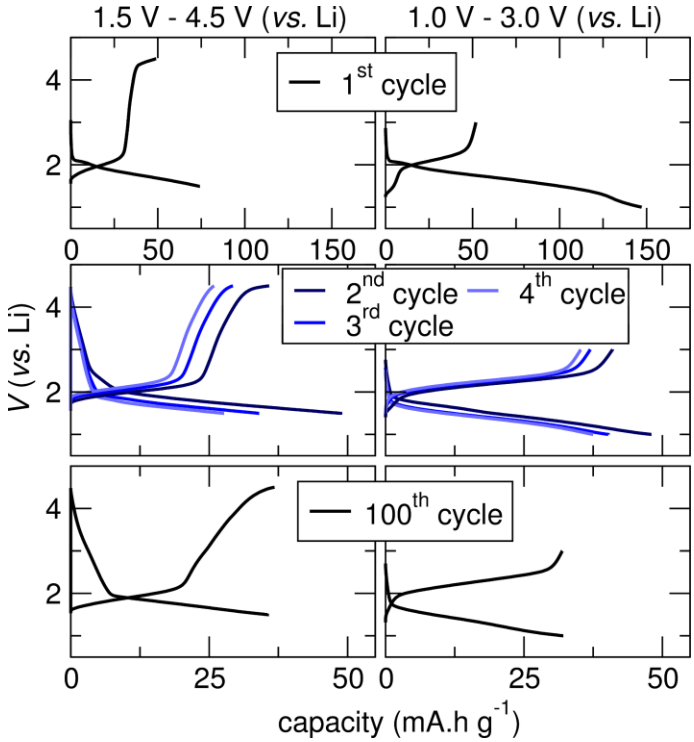

Figure S9. The discharge and charge profiles of *bipy*-CTF-400 when cycled between (left column) 1.5 V – 4.5 V (*vs.* Li) and (right column) 1.0 V – 3.0 V (*vs.* Li). All cells are cycled at 0.1 A g^{-1}. Decreasing the discharge cutoff voltage does not increase the capacity after the 1st cycle suggesting irreversible Faradaic processes are occurring below 1.5 V.

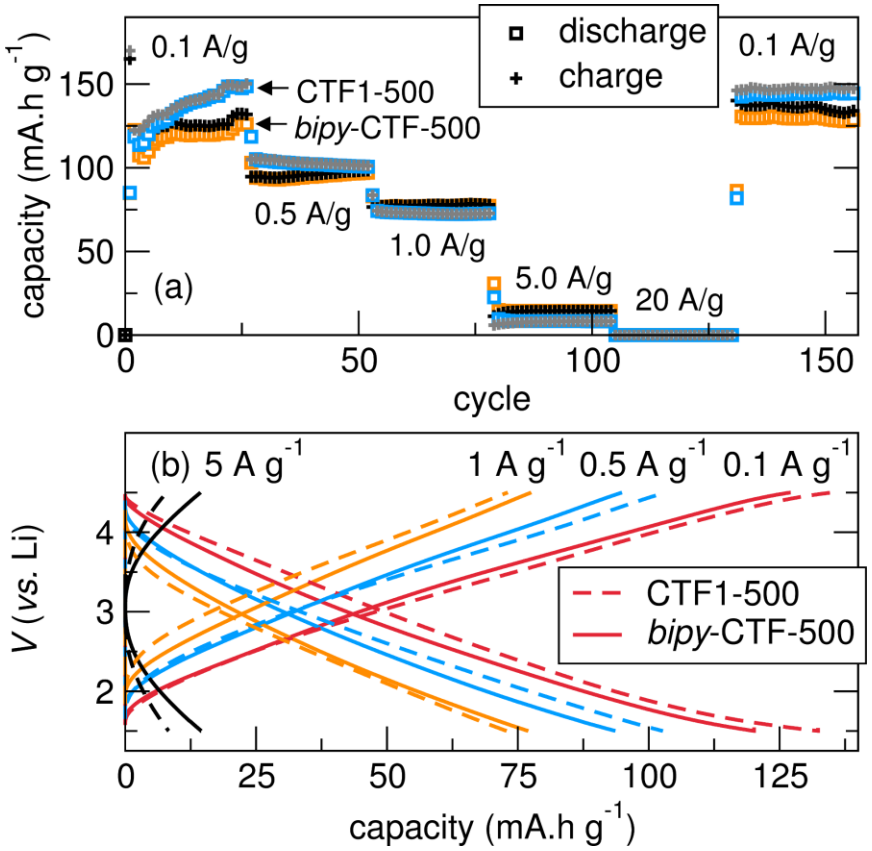

Figure S10. (a) The charge storage capabilities of CTF1 and *bipy*-CTF materials prepared at 500 °C show a dependence on the rate suggesting a kinetically limited process. (b) The discharge and charge profiles exhibit large internal resistance drops when cycled at higher rates suggesting that the cell configuration is causing the lowered capacity.

References

(1) Bojdys, M. J.; Müller, J.-O.; Antonietti, M.; Thomas, A. Ionothermal Synthesis of Crystalline, Condensed, Graphitic Carbon Nitride. *Chem. – Eur. J.* **2008**, *14* (27), 8177–8182.

(2) Wirnhier, E.; Döblinger, M.; Gunzelmann, D.; Senker, J.; Lotsch, B. V.; Schnick, W. Poly(triazine Imide) with Intercalation of Lithium and Chloride Ions $[(C_3N_3)_2(NH_xLi_{1-x})_3 \cdot LiCl]$: A Crystalline 2D Carbon Nitride Network. *Chem. – Eur. J.* **2011**, *17* (11), 3213–3221.

(3) Schwinghammer, K.; Tuffy, B.; Mesch, M. B.; Wirnhier, E.; Martineau, C.; Taulelle, F.; Schnick, W.; Senker, J.; Lotsch, B. V. Triazine-Based Carbon Nitrides for Visible-Light-Driven Hydrogen Evolution. *Angew. Chem. Int. Ed.* **2013**, *52* (9), 2435–2439.